Dynamics of coupled oscillator systems in presence of a local potential

Alessandro Campa[1] and Shamik Gupta[2]

[1] *Complex Systems and Theoretical Physics Unit, Health and Technology Department, Istituto Superiore di Sanità, and INFN Roma1, Viale Regina Elena 299, 00161 Roma, Italy*
[2] *Max Planck Institute for the Physics of Complex Systems, Nöthnitzer Straße 38, 01187 Dresden, Germany*

arXiv:1610.04037v2 [nlin.AO] 19 Dec 2016

PACS 05.45.Xt – Synchronization; coupled oscillators
PACS 05.70.Fh – Phase transitions: general studies
PACS 05.70.Ln – Nonequilibrium and irreversible thermodynamics

Abstract –We consider a long-range model of coupled phase-only oscillators subject to a local potential and evolving in presence of thermal noise. The model is a non-trivial generalization of the celebrated Kuramoto model of collective synchronization. We demonstrate by exact results and numerics a surprisingly rich long-time behavior, in which the system settles into either a stationary state that could be in or out of equilibrium and supports either global synchrony or absence of it, or, in a time-periodic synchronized state. The system shows both continuous and discontinuous phase transitions, as well as an interesting reentrant transition in which the system successively loses and gains synchrony on steady increase of the relevant tuning parameter.

Introduction. – The issue of how self-sustained oscillators of widely different natural frequencies when interacting *weakly* with one another may *spontaneously* oscillate at a common frequency has intrigued researchers since one of its first documented observations by the Dutch physicist Christiaan Huygens in the 17th century. This phenomenon of collective synchrony is commonly observed in nature, e.g., in metabolic synchrony in yeast cell suspensions [1], among groups of fireflies that flash in unison [2], in animal flocking behavior [3], and perhaps most importantly of all, in cardiac pacemaker cells whose synchronized firings keep the heart beating and life going on [4]. Synchrony is much desired in man-made systems, e.g., in parallel computing in computer science, whereby processors must coordinate to finish a task on time, and in electrical power-grids constituting generators that must run in synchrony so as to be tuned in frequency to that of the grid [5,6]. However, synchrony could also be hazardous, e.g., in neurons, leading to impaired brain function in Parkinson's disease and epilepsy. For an overview, see Refs. [7, 8].

Over the years, the celebrated Kuramoto model has served as a paradigmatic model to study analytically the emergence of synchrony in many-oscillator systems [9]; for a review, see Refs. [10–12]. The model comprises N phase-only oscillators of distributed natural frequencies that are globally coupled through the sine of their phase differences. The ith oscillator, $i = 1, 2, \ldots, N$, has its phase $\theta_i \in [0, 2\pi)$ evolving according to the equation

$$\frac{\mathrm{d}\theta_i}{\mathrm{d}t} = \omega_i + \frac{K}{N}\sum_{j=1}^{N}\sin(\theta_j - \theta_i), \tag{1}$$

where ω_i is the natural frequency of the ith oscillator. Here, $K > 0$ is the coupling constant, and the second term on the right hand side (rhs) describes an attractive all-to-all interaction between the oscillators, with the factor $1/N$ making the model well behaved in the limit $N \to \infty$.

For a given frequency distribution $g(\omega)$ common to all, the tendency of each oscillator to oscillate independently at its own natural frequency is opposed by the global coupling among them. Indeed, the latter favors equal phases for the oscillators, $\theta_i = \theta_j \ \forall \ i \neq j$, thereby promoting global synchrony in which all the oscillator phases turn around in time at a common frequency given by the mean Ω of the distribution $g(\omega)$. A measure of the amount of synchrony in the system is given by the order parameter $r \equiv |\mathbf{r}| = \sqrt{r_x^2 + r_y^2}$, where the vector $\mathbf{r}$ is given by $\mathbf{r} = (r_x, r_y) \equiv \sum_{j=1}^{N}(\cos\theta_j, \sin\theta_j)/N$ [9].

The Kuramoto model has been mostly studied for a unimodal $g(\omega)$, i.e., one that is symmetric about the mean Ω, and which decreases monotonically to zero with increasing $|\omega - \Omega|$. In this case, it has been shown that for a

given K and in the limit $N \to \infty$, on tuning the width σ of $g(\omega)$, the dynamics at long times favors a synchronized phase ($r \neq 0$) at low σ, and an unsynchronized phase ($r = 0$) at high σ, with a continuous transition between the two phases at the critical value $\sigma_c \equiv \pi K g_1(\Omega)/2$ [10–12], where g_1 is the distribution obtained from g by setting in the latter the width to unity.

Several extensions of the Kuramoto model have been studied, including the case with inertia for which the dynamics of phases is governed by second-order equations in time (see Ref. [12] for a review). The main purpose of these studies has been to investigate the robustness of synchronization properties and change in their characteristics, as well as in the thermodynamic phase diagram, in models that may reproduce realistic systems. A natural extension considered in this paper is represented by the presence of a local potential acting as a torque on each oscillator.

Model and main results. – In this paper, we consider the case of identical oscillators, $g(\omega) = \delta(\omega - \Omega)$, in the Kuramoto model, with an additional thermal noise and a local potential acting on the individual oscillators. The underlying equation of motion is

$$\frac{\mathrm{d}\theta_i}{\mathrm{d}t} = \Omega + \frac{K}{N}\sum_{j=1}^{N}\sin(\theta_j - \theta_i) - W\sin 2\theta_i + \eta_i(t), \quad (2)$$

where the third term on the rhs describes a torque due to a local potential $-(W/2)\cos(2\theta_i)$, with $W \geq 0$ quantifying its strength, while $\eta_i(t)$ is a Gaussian, white noise, with $\langle \eta_i(t) \rangle = 0$, $\langle \eta_i(t)\eta_j(t') \rangle = 2T\delta_{ij}\delta(t-t')$. The temperature T is measured in units of the Boltzmann constant, while angular brackets denote averaging over noise realizations.

The thermal noise may be interpreted as the effect of a coupling to the external environment [12], but may also be seen as accounting for stochastic fluctuations of the natural frequencies in time [13]. The local potential alone, which has its minima at $\theta = 0$ and $\theta = \pi$, tends to "pin" the θ's to these values, thus playing the role of a pinning potential, as was considered in Ref. [14]. The latter work investigated the case of the pinning potential $\sim \sin(\alpha_i - \theta_i)$ that tends to pin the phase of the ith oscillator to the corresponding *random* pinning angle α_i. With every oscillator pinned to a random angle, such a pinning potential evidently favors a static, *disordered* arrangement of the phases. By contrast, the pinning potential in our case favors a static, *ordered* arrangement of the phases.

We now remark on some known limits of the dynamics (2). For $W = T = 0$, the dynamics reduces to that of the Kuramoto model (1), in the particular case of the latter in which all the oscillators have the same frequency. In this work, we consider $T > 0$. For $\Omega = W = 0$, Eq. (2) describes the overdamped dynamics of the so-called Brownian mean-field model [15]. The latter model was introduced as a generalization of the energy-conserving microcanonical dynamics of the Hamiltonian mean-field (HMF) model [16], a paradigmatic system to study static and dynamic properties of long-range interacting (LRI) systems[1], to the situation where the system exchanges energy by interacting with a heat bath.

For $\Omega \neq 0$ (respectively, $\Omega = 0$), the dynamics (2) relaxes at long times to a non-equilibrium stationary state (NESS) (respectively, equilibrium). Unlike equilibrium, NESSs do not respect detailed balance and support fluxes of conserved quantities in the system. Studying NESSs constitutes an active area of research in modern statistical mechanics, where a challenge is to achieve a level of understanding akin to the one established for equilibrium systems [20]. The local potential term in Eq. (2) does not allow to get rid of the effect of the natural frequency by studying the dynamics in a frame rotating uniformly with frequency Ω, thereby recovering equilibrium dynamics, as is possible with $W = 0$ [12].

The Kuramoto model (1) subject to a periodic forcing $F\sin(\sigma t - \theta_i)$ has been studied in Refs. [13, 21, 22] to address the issue of forced synchronization. The governing equation when viewed in the frame rotating with the forcing frequency σ reads $\mathrm{d}\theta_i/\mathrm{d}t = \omega_i - \sigma + (K/N)\sum_{j=1}^{N}\sin(\theta_j - \theta_i) - F\sin\theta_i$. Comparing with Eq. (2), one immediately realizes the differences: in our model, all the oscillators have the same intrinsic frequency Ω, the parameter $\sigma = 0$, there is thermal noise, and moreover, the additional term instead of being $-\sin\theta_i$ is $-\sin 2\theta_i$. The Kuramoto model (1) with an additional external drive f_e and a pinning potential $-a\cos\theta_i + (b/2)\cos 2\theta_i$ on the rhs has been studied in Ref. [23] to discuss how an ensemble of noiseless globally-coupled pinned oscillators with distributed intrinsic frequencies is capable of rectifying spatial disorder, thus acting as a rectifier [24], and exhibiting the phenomenon of absolute negative mobility [25]. In contrast to this model, our model has all the oscillators with the same intrinsic frequency (as we comment below, this implies that the current has always the same sign as that of the external drive Ω), and furthermore, it has stochastic noise in it.

Before proceeding with an analysis of the model (2), we first set $K = 1$ without loss of generality, and discuss the dynamical features and expected behavior of the model at long times. Consider first the low-T limit of the dynamics. In the absence of the local potential (i.e., with $W = 0$), the system goes to a trivially synchronized state[2]. Namely, it reduces to the Kuramoto model with identical frequency Ω of the oscillators. Correspondingly, the order parameter r is close to unity, but the vector $\mathbf{r}$ varies *periodically in time* with period Ω. On the other hand, with $W > 0$ and $\Omega = 0$, the following occurs. As mentioned above, the local potential alone tends to make the θ's crowd around $\theta =$

[1] Long-range interacting (LRI) systems are those in which the inter-particle potential decays slowly with the separation r as $r^{-\alpha}$ for large r, with $0 \leq \alpha < d$ in d spatial dimensions [17–19].

[2] In the following, we use interchangeably the terms "state" and "phase" to mean an ensemble of microscopic configurations distributed with a given density.

$0, \pi$, while the global coupling alone tends to make $\theta_i = \theta_j \; \forall \; i, j$. Thus, together, and in the absence of the natural frequency term, the two terms lead to a static arrangement of θ's around either 0 or π, resulting at long times in a stationary state that is fully synchronized. This tendency is opposed by the frequency term that tends to drive the phases at a constant angular velocity Ω, thus leading, for sufficiently large Ω, to a time-periodic synchronized state. Increasing the temperature results in enhanced thermal fluctuations that tend to destroy synchrony, be it in the stationary or in the time-periodic state. The interplay between these competing tendencies leads to a surprisingly rich phase diagram, as we demonstrate below.

Specifically, we show that the system settles into either a stationary state that could be in equilibrium or in a NESS and may or may not support global synchrony, or, in a time-periodic synchronized state. In presence of noise and other competing aspects of the dynamics, in the latter state the order parameter r is not constant in time but shows time-periodic oscillations. We also show that the system exhibits both continuous and discontinuous transitions between different phases, as well as an interesting reentrant transition in which the system successively loses and gains synchrony on steady increase of the relevant tuning parameter. It is remarkable that in the absence of a general framework to study NESSs akin to the one due to Boltzmann and Gibbs for equilibrium states, our tools and analysis allow to obtain *exact* analytical results for the NESSs of the nontrivial dynamics (2).

We remark that in terms of the (r_x, r_y), Eq. (2) becomes

$$\frac{\mathrm{d}\theta_i}{\mathrm{d}t} = \Omega - r_x \sin\theta_i + r_y \cos\theta_i - W \sin 2\theta_i + \eta_i(t), \quad (3)$$

which makes it evident that the dynamics is effectively that of a single oscillator evolving in a self-consistent mean field of strength r produced by all the oscillators; the parameters characterizing the dynamics are Ω, T, W.

Analysis in the limit $N \to \infty$ and the stationary state. – In the limit $N \to \infty$, the state of the system is characterized by the single-oscillator distribution $f(\theta, t)$, defined such that $f(\theta, t)\mathrm{d}\theta$ gives the probability at time t that a randomly chosen oscillator has its phase between θ and $\theta + \mathrm{d}\theta$. One has $f(\theta + 2\pi, t) = f(\theta, t)$, and the normalization $\int_0^{2\pi} \mathrm{d}\theta \, f(\theta, t) = 1 \; \forall \; t$. The time evolution of $f(\theta, t)$ is given by the Fokker-Planck (FP) equation that may be straightforwardly written down from Eq. (3):

$$\frac{\partial f}{\partial t} = -\frac{\partial[(\Omega - r_x \sin\theta + r_y \cos\theta - W \sin 2\theta) f]}{\partial \theta} + T \frac{\partial^2 f}{\partial \theta^2}, \quad (4)$$

where r_x, r_y are now functionals of $f(\theta, t)$: $(r_x, r_y) \equiv (r_x, r_y)[f] = \int \mathrm{d}\theta \, (\cos\theta, \sin\theta) f(\theta, t)$. When exists, the stationary solution of Eq. (4) is obtained by setting the left hand side (lhs) to zero; the solution reads [12,13]

$$f(\theta) = B e^{\frac{v(\theta)}{T}} \left[1 + (e^{-2\pi\Omega/T} - 1) \frac{\int_0^\theta \mathrm{d}\theta' \, e^{-\frac{v(\theta')}{T}}}{\int_0^{2\pi} \mathrm{d}\theta' \, e^{-\frac{v(\theta')}{T}}} \right], \quad (5)$$

with $v(\theta) \equiv v[f](\theta) = \Omega\theta + r_x \cos\theta + r_y \sin\theta + (W/2)\cos 2\theta$, while the constant B is fixed by the normalization of $f(\theta)$. The stationary quantities $r_{x,y}$ are determined self-consistently:

$$(r_x, r_y) \equiv \int \mathrm{d}\theta \, (\cos\theta, \sin\theta) f(\theta). \quad (6)$$

The stationary unsynchronized solution $f_0(\theta)$ with $r_x = r_y = 0$ always exists, but it may be unstable in regions of the parameter space (Ω, T, W); Eq. (5) yields

$$f_0(\theta) = B e^{\frac{v_0(\theta)}{T}} \left[1 + (e^{-2\pi\Omega/T} - 1) \frac{\int_0^\theta \mathrm{d}\theta' \, e^{-\frac{v_0(\theta')}{T}}}{\int_0^{2\pi} \mathrm{d}\theta' \, e^{-\frac{v_0(\theta')}{T}}} \right], \quad (7)$$

with $v_0(\theta) \equiv v_0[f](\theta) = \Omega\theta + (W/2)\cos 2\theta$. For $W = 0$, one has the homogeneous distribution, $f_0(\theta) = 1/(2\pi)$, but for $W > 0$, although unsynchronized, $f_0(\theta)$ is *not* homogeneous in θ. As mentioned earlier, one has an equilibrium stationary state for $\Omega = 0$ (i.e., on the (T, W)-plane), and a NESS for $\Omega \neq 0$.

One may define a current $J \equiv \langle\dot{\theta}\rangle/(2\pi)$ [23], to characterize the motion of the oscillator phases. Summing Eq. (3) over i and averaging over noise gives $J(t) = [\Omega - W\langle\sin 2\theta\rangle(t)]/(2\pi)$. In the stationary state, the stationary current J_{st} is obtained from Eq. (5) as $J_{\mathrm{st}} = BT[1 - e^{-2\pi\Omega/T}] / \int_0^{2\pi} d\theta' \, e^{-v(\theta')/T}$, which implies zero current for $\Omega = 0$; this is expected since in this case, the system is in equilibrium. Also, for $\Omega \neq 0$, when the system is in a NESS, we have that J_{st} has the same sign as that of Ω. Note that these features hold irrespective of whether the stationary state is synchronized or unsynchronized. In the time-periodic state, the current is obtained either from the equations of motion (3) or by using the Fokker-Planck equation (4).

Linear stability of the stationary unsynchronized state. – Let us now study the linear stability of the stationary unsynchronized state $f_0(\theta)$. To this end, we linearize Eq. (4) around $f_0(\theta)$, by writing $f(\theta, t) = f_0(\theta) + \delta f(\theta, t)$; $|\delta f| \ll 1$, and keeping the zeroth and first-order terms in δf. The zeroth-order terms cancel; the first-order terms give

$$\frac{\partial \delta f}{\partial t} = -\frac{\partial}{\partial \theta} [(\Omega - W \sin 2\theta) \delta f] + \frac{\partial}{\partial \theta} [(r_x \sin\theta - r_y \cos\theta) f_0(\theta)] + T \frac{\partial^2 \delta f}{\partial \theta^2}, \quad (8)$$

with $(r_x, r_y) = \int \mathrm{d}\theta \, (\cos\theta, \sin\theta) \delta f(\theta, t)$. Now, $f_0(\theta)$ is stable if the eigenvalue spectrum of the linear operator $\mathcal{L}$ defined by the rhs of Eq. (8) has a negative real part.

To study the linear problem, we compute the matrix elements $\mathcal{L}_{k',k}$ of $\mathcal{L}$ with respect to the set of complete basis constituted by the functions $\exp(ik\theta)$, with k an integer, for functions in $[0, 2\pi)$. Using Eq. (8), we have

$$\begin{aligned}\mathcal{L}_{k',k} &\equiv \frac{1}{2\pi}\int_0^{2\pi} \mathrm{d}\theta\, e^{-ik'\theta}\mathcal{L}e^{ik\theta} \\ &= -(ik\Omega + k^2T)\delta_{k',k} + \frac{ik'W}{2\pi}\int \mathrm{d}\theta\, \sin 2\theta e^{i(k-k')\theta} \\ &+\frac{ik'}{2\pi}\int \mathrm{d}\theta\, \left[r_x \sin\theta - r_y\cos\theta\right] f_0(\theta)e^{-ik'\theta}, \end{aligned} \tag{9}$$

with $(r_x, r_y) = \int \mathrm{d}\theta\,(\cos\theta, \sin\theta)e^{ik\theta}$. Using the relations $\int \mathrm{d}\theta\, \cos\theta e^{ik\theta} = \pi(\delta_{k,1} + \delta_{k,-1})$, $\int \mathrm{d}\theta\, \sin\theta e^{ik\theta} = i\pi(\delta_{k,1} - \delta_{k,-1})$, $\int \mathrm{d}\theta\, \sin 2\theta e^{ik\theta} = i\pi(\delta_{k,2} - \delta_{k,-2})$ in Eq. (9) gives

$$\begin{aligned}\mathcal{L}_{k',k} &= -(ik\Omega + k^2T)\delta_{k',k} + \frac{W}{2}k'(\delta_{k',k+2} - \delta_{k',k-2}) \\ &+\frac{ik'}{2}\int \mathrm{d}\theta \Big[(\delta_{k,1} + \delta_{k,-1})\sin\theta \\ &-i(\delta_{k,1} - \delta_{k,-1})\cos\theta\Big] f_0(\theta)e^{-ik'\theta}. \end{aligned} \tag{10}$$

Using $\sin\theta \pm i\cos\theta = \pm ie^{\mp i\theta}$, and introducing the Fourier components of $f_0(\theta)$, $\widetilde{f}_p \equiv \int_0^{2\pi} \mathrm{d}\theta\, e^{-ip\theta} f_0(\theta)$, we arrive at the following final expression of the matrix elements:

$$\begin{aligned}\mathcal{L}_{k',k} &= -(ik\Omega + k^2T)\delta_{k',k} + \frac{W}{2}k'(\delta_{k',k+2} - \delta_{k',k-2}) \\ &+\frac{k'}{2}\left[\delta_{k,1}\widetilde{f}_{k'-1} - \delta_{k,-1}\widetilde{f}_{k'+1}\right]. \end{aligned} \tag{11}$$

For $W = 0$, we have $f_0(\theta) = 1/(2\pi)$, giving $\widetilde{f}_p = \delta_{p,0}$, so that the matrix becomes diagonal,

$$\mathcal{L}_{k',k} = \left[-ik\Omega - k^2T + \frac{1}{2}(\delta_{k,1} + \delta_{k,-1})\right]\delta_{k',k}, \tag{12}$$

which readily gives the eigenvalues. Before proceeding, let us adopt the following order for the rows and columns of the matrix. The indices k, k' take integer values; we order the indices according to $k, k' = 0, 1, -1, 2, -2, 3, -3, \ldots$. With this ordering, we see that all elements of the first row of the matrix vanish, i.e., $\mathcal{L}_{0,k} = 0\ \forall\ k$. In the first column, only two elements do not vanish: $\mathcal{L}_{2,0} = \mathcal{L}_{-2,0} = W$.

Now, the order of the matrix $\mathcal{L}$ being infinite, we consider in the following the matrix of a finite size obtained by truncating the infinite one at a given maximum value $k = k_{\max}$; the order of this finite matrix is $2k_{\max} + 1$. We study the eigenvalues of this truncated matrix; we have chosen a value for $k_{\max}$ that is large enough that our results, as far as the determination of stability is concerned, do not change for larger $k_{\max}$. Since the elements in the first row of the matrix vanish, there is always a zero eigenvalue; however, the stability of $f_0(\theta)$ is determined by the other eigenvalues, i.e., $f_0(\theta)$ is stable if the real part of all the other eigenvalues is negative, while it is unstable if there is at least one eigenvalue with a positive real part.

To see that the zero eigenvalue may be disregarded, we reason as follows. Since the original FP equation conserves the normalization of f, and $f_0(\theta)$ is normalized, we have to study the linearized equation (8) for functions $\delta f(\theta, t)$ that satisfy $\int_0^{2\pi} \mathrm{d}\theta\, \delta f(\theta, t) = 0\ \forall\ t$. Now, the eigenfunction δf corresponding to the zero eigenvalue is obtained directly from Eq. (8) by setting the lhs to zero. From the definition of $f_0(\theta)$, we see that this linear equation is solved by $\delta f(\theta) \propto f_0(\theta)$. Since $f_0(\theta)$ is positive definite, such a δf has a non-vanishing integral over $[0, 2\pi)$ (thus, it has a nonzero Fourier component for $k = 0$), and is therefore not suitable for our stability problem. On the other hand, each eigenfunction δf corresponding to a non-vanishing eigenvalue must have a zero Fourier component for $k = 0$: in fact, $\sum_k \mathcal{L}_{0,k}a_k = 0$ for any vector a_k, as we have seen, then this cannot be equal to λa_0 if both λ and a_0 are different from 0. In conclusion, any non-vanishing eigenvalue of the matrix $\mathcal{L}$ has a corresponding eigenfunction whose first component (i.e., that corresponding to $k = 0$), is 0, and thus, it belongs to the class suitable for our stability problem. This also implies, as a byproduct, that the matrix $\mathcal{L}$ and the matrix of order $2k_{\max}$ obtained by deleting the first row and the first column of $\mathcal{L}$ have the same non-vanishing eigenvalues.

Summarizing, $f_0(\theta)$ is stable if all the non-vanishing eigenvalues of $\mathcal{L}$ have a negative real part. For our computations, for any chosen values of (T, W), we vary Ω, and compute numerically the eigenvalues of $\mathcal{L}$, thus determining the parameter regimes where f_0 is stable. When f_0 is unstable, the system may settle into a synchronized state that is either stationary or time-periodic.

Linear stability of the stationary synchronized state. – We now discuss how to obtain the linear stability threshold of the synchronized state (5). This threshold should be computed by linearizing the Fokker-Planck equation (4) about the state (5), along the lines followed above to compute the stability threshold of the unsynchronized state. Given the complexity of the state (5), such a task turns out to be quite formidable, and, hence, we resort to a different strategy, as detailed below.

To compute the threshold for given values of T and W, we vary Ω, and obtain numerically the corresponding non-zero values of r_x and r_y that satisfy the self-consistent equations (6). Operatively, this is done as follows. For $\Omega = 0$, the corresponding non-zero r_x is easily found numerically, while one has $r_y = 0$. Then, for $\Omega > 0$, we increase Ω in small steps of size $\mathrm{d}\Omega$, and compute correspondingly the new values of r_x and r_y after every step by using the partial derivatives of $f(\theta; T, W, \Omega, r_x, r_y)$ with respect to the parameters. Here, we have written explicitly the parameters on which the solution (5) depends, as $f(\theta; T, W, \Omega, r_x, r_y)$ (the normalizing factor B then also depends on the parameters). Having reached the Ω value corresponding to the stability threshold of the synchronized state is signaled by the fact that the above procedure does not find any more non-zero r_x and r_y.

Figure 1(a) shows representative results of our analytic computation, in which (i) the red line indicates loss of stability of the stationary unsynchronized state $f_0(\theta)$ and transition to the stationary synchronized state at smaller Ω, (ii) the blue line indicates loss of stability of the stationary synchronized state (5), and consequently, a transition at larger Ω either to the stationary unsynchronized state or to the time-periodic state (see below the different cases), and (iii) the green line indicates loss of stability of the stationary unsynchronized state $f_0(\theta)$ and transition to the time-periodic state at larger Ω. Our computation indicates that the red and green lines emerge from a common point $C = C(\Omega, W, T)$, while the blue line starts at the origin ($\Omega = W = 0$), extending in a region where the red and green lines do not exist. In this latter region, the blue line corresponds to a transition between the stationary synchronized and the time-periodic state. This transition may not be called a phase transition since the latter is usually meant to refer to a transition between two states that are both stationary, besides having different macroscopic properties. The red and blue lines eventually merge with one another, see Fig. 1(a). The point C approaches the origin ($\Omega = W = 0$) as T approaches $1/2$ from below; concomitantly, the green line approaches the Ω-axis, while the red line becomes more inclined towards the W-axis, approaching the blue line and disappearing for $T > 1/2$; this suggests that for $T \geq 1/2$, the late-time dynamics does not support a time-periodic state.

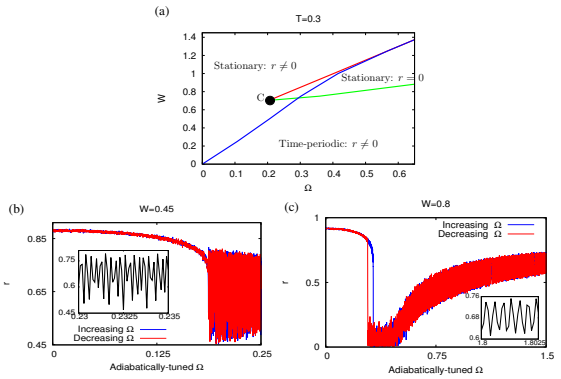

Fig. 1: (a) Phase diagram in the (Ω, W)-plane for $T = 0.3$. Here, the red line (respectively, the green line) corresponds to loss of stability of the stationary unsynchronized state and transition to the stationary synchronized state (respectively, the time-periodic state) at smaller (respectively, larger) Ω. The blue line refers to the stability threshold of the stationary synchronized state. (b),(c): Numerical simulation results for r vs. adiabatically-tuned Ω. The system size is $N = 10^4$. Panel (b) corresponds to a value of W lower than the one corresponding to the point C in (a). Panel (c) refers to a value of W larger than the one corresponding to the point C, and specifically, to a value of W at which on increasing Ω, the green line in (a) is met after the blue line. The insets in panels (b) and (c) demonstrate time-periodic behavior of r in the relevant Ω-regime.

We now report on numerical simulations of the dynamics[3]. At fixed values of (W, T), we perform two sets of simulations. In one set, we start at $\Omega = 0$ from a state with $r = 1$, prepared by setting $\theta_i = 0\ \forall\ i$, and then tune Ω adiabatically to a large-enough value, while simultaneously monitoring r as a function of Ω. In the other set, we start with the state obtained as the final state of the first set of simulations, and then adiabatically decrease Ω to zero. Adiabatic tuning of Ω ensures that the system has sufficient time to attain stationarity before the value of Ω changes significantly. The results of simulations are displayed in Fig. 1, panels (b) and (c) at a temperature below $1/2$, namely, $T = 0.3$. We now discuss in detail the results presented in these panels.

Figure 1(b) corresponds to a value of W lower than the one corresponding to the point C; we note that consistent with the phase diagram in (a), the system goes over from the stationary synchronized to the time-periodic state by crossing the blue line in (a).

Figure 1(c) refers to a value of W larger than the one corresponding to the point C, and specifically, to a value at which on increasing Ω, the green line in (a) is met after the blue line. The results show that consistent with our computation, on increasing Ω, the system goes over from the stationary synchronized to the stationary unsynchronized state (corresponding to crossing of the blue line in (a)), and then goes over to the time-periodic synchronized state (corresponding to crossing of the green line in (a)). Subsequently, on decreasing Ω, the system goes over to the stationary unsynchronized state by crossing the green line in (a) and then to the stationary synchronized state by crossing the red line in (a). This behavior suggests that while the transition between the stationary synchronized and the stationary unsynchronized state is discontinuous (as evidenced by the presence of a hysteresis loop in (c)), the one between the stationary unsynchronized and the time-periodic state is continuous (implied by the absence of any hysteresis loop in (c)). We see from Fig. 1(c) the emergence of a feature induced by the local potential, which is absent in the Kuramoto model, namely, that of a reentrant transition in which the system successively loses and gains synchrony on steady increase of Ω. Similar reentrant transitions between states that are stationary (unlike our case where one state is time-periodic) are observed in the version of the Kuramoto model that includes a phase lag in the coupling and inertial effects [26,27].

Let us now discuss the situation for a value of W larger than, but close to, the one corresponding to the point C, and specifically, to a value at which on increasing Ω, the green line in Fig. 1(a) is met before the blue line. Here, on increasing Ω, the system goes over from the stationary synchronized to the time-periodic state on crossing the blue line in (a) (note that no change in behavior is expected on crossing the green line in (a) while starting from the state $r = 1$ and then adiabatically increasing Ω.)

[3] All numerical simulations reported in this paper involved employing a first-order Euler algorithm to integrate the equation of motion (2), with timestep $\mathrm{d}t = 0.01$.

On decreasing Ω, the time-periodic state goes over to the stationary unsynchronized state on crossing the green line in (a) and then to the stationary synchronized state on crossing the red line in (a).

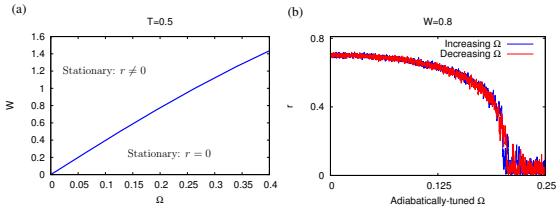

Fig. 2: (a) Phase diagram in the (Ω, W)-plane for $T = 0.5$. The blue line refers to the line of continuous transition between the stationary synchronized and unsynchronized states. (b) Numerical simulation results for r as a function of adiabatically-tuned Ω at a representative W. The system size is $N = 10^4$.

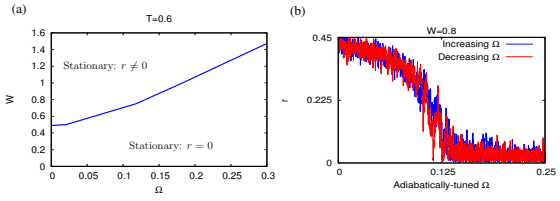

Fig. 3: (a) Phase diagram in the (Ω, W)-plane for $T = 0.6$. The blue line refers to a continuous transition between the stationary synchronized and unsynchronized states. (b) Numerical simulation results for r as a function of adiabatically-tuned Ω at a representative value of W above the minimum of the blue line in (a) (that occurs at $\Omega = 0$); for W values below this minimum, r is equal to zero at all Ω. The system size is $N = 10^4$.

Till now we have discussed the behavior of our model for $T < 1/2$. For $T \geq 1/2$, our analysis presented below shows that one has a continuous transition between the stationary synchronized and the stationary unsynchronized state (we have already discussed that the time-periodic state disappears as T approaches $1/2$ from below).

Continuous transition points between the stationary synchronized and unsynchronized states. – For the determination of points of continuous transition where the stationary unsynchronized state (7) becomes synchronized, we adopt the usual strategy of expanding to first order the self-consistent equation of the order parameter. The two self-consistent equations (6) are rewritten as

$$(r_x, r_y) = \int \mathrm{d}\theta \, (\cos\theta, \sin\theta) \; f(\theta; T, W, \Omega, r_x, r_y). \quad (13)$$

We now make an expansion of the function f around $r_x = r_y = 0$. Denoting with a subscript the partial derivatives of f with respect to the parameters, we then write

$$f(\theta; T, W, \Omega, r_x, r_y) = f(\theta; T, W, \Omega, 0, 0) \quad (14)$$
$$+ f_{r_x}(\theta; T, W, \Omega, 0, 0) r_x + f_{r_y}(\theta; T, W, \Omega, 0, 0) r_y + O(r^2).$$

Since the integral of either $\cos\theta$ or $\sin\theta$ multiplied by $f(\theta; T, W, \Omega, 0, 0)$ vanishes, plugging the last expansion in Eq. (13), and defining $C_{xx} \equiv \int \mathrm{d}\theta \cos\theta \; f_{r_x}(\theta)$, $C_{xy} \equiv \int \mathrm{d}\theta \cos\theta \; f_{r_y}(\theta), C_{yx} \equiv \int \mathrm{d}\theta \sin\theta \; f_{r_x}(\theta), C_{yy} \equiv \int \mathrm{d}\theta \sin\theta \, f_{r_y}(\theta)$, (the parameters $(T, W, \Omega, 0, 0)$ in f_{r_x} and f_{r_y} are not displayed for visual clarity) the self-consistent equations may be written as

$$C_{xx} r_x + C_{xy} r_y = r_x, \; C_{yx} r_x + C_{yy} r_y = r_y. \quad (15)$$

This system of equations has nontrivial solutions when the matrix C has an eigenvalue equal to 1, i.e., when $\det(C - I) = 0$, with I the identity matrix. The latter condition gives an equation in (Ω, T, W) the solution of which gives the surface of continuous transition in the parameter space. The line in the (T, W)-plane given by the intersection of this surface is the line of critical points between equilibrium states (since $\Omega = 0$). In this case, the solution (5) becomes $f(\theta; T, W, 0, r_x, 0)) = B \exp[(r_x \cos\theta + (W/2)\cos 2\theta)/T]$, since $r_y = 0$, and the points of continuous transition are given by $C_{xx} = 1$.

The results of our computation are shown by blue lines in panel (a) of Figs. 2 and 3 for $T = 0.5$ and $T = 0.6$, respectively. Numerical simulation results for r as a function of adiabatically-tuned Ω, displayed in the other panels of these figures, show the absence of a hysteresis loop characteristic of a discontinuous transition, but rather a variation that coincides, up to fluctuations due to finite N and thermal noise, for increasing and decreasing Ω. This observation supports our claim that the system undergoes a continuous transition between the stationary synchronized and the stationary unsynchronized state on crossing the blue line in (a) of Figs. 2 and 3.

We note that for our model, the current J is always positive for $\Omega > 0$. In the stationary state, J_{st} increases with Ω independently from the synchronization property of the state. In the time-periodic states, J is obviously periodic, with its average over a period increasing with Ω.

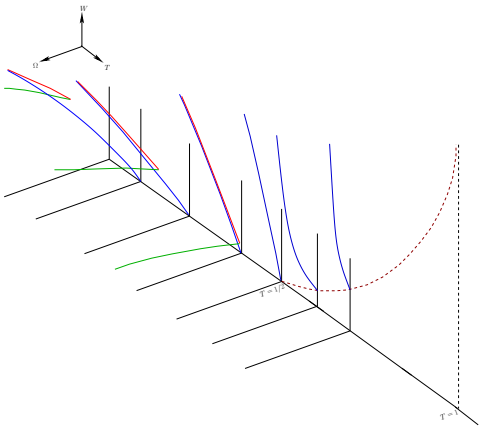

Fig. 4: Schematic phase diagram in the (Ω, T, W) space, specifically, on a set of (Ω, W)-planes for increasing values of T.

Based on our results, we show in Fig. 4 a schematic phase diagram of our model in the (Ω, T, W) space. Note

the point of continuous transition for $\Omega = W = 0$ given by $T = T_c = 1/2$, which coincides with the phase transition point for the BMF model to which the dynamics (2) reduces under these limiting values of Ω and W. With respect to Fig. 4, one may wonder as to how for $T \geq 1/2$ does the point of intersection of the blue line of continuous transition with the (W, T)-plane (i.e., $\Omega = 0$) behave as a function of T. We now show that this point, which starts at $(T = 1/2, W = 0)$, has the limiting value $(T = 1, W \to \infty)$, see the brown dotted line on the (T, W)-plane in Fig. 4. In the limit $W \to \infty$, the oscillator phases have only two allowed values, $\theta = 0$ and $\theta = \pi$, thus, $\cos\theta$ can be either $+1$ or -1. This implies that $r_y = 0$, while $r = r_x$ may be easily computed by noting that for $\Omega = 0, W \to \infty$, the dynamics has the Gibbs-Boltzmann equilibrium stationary state: $f(\theta = 0) \propto \exp(r_x/T)$ and $f(\theta = \pi) \propto \exp(-r_x/T)$. We thus have $r = \tanh(r/T)$. This transcendental equation has a non-zero solution for r provided $T \leq 1$, giving the critical temperature of transition as unity.

Conclusions and perspectives. – In this paper, we studied a model system of globally-coupled oscillators with an additional local potential acting on the individual oscillators, and evolving in presence of thermal noise. We demonstrated by exact results and numerics a surprisingly rich long-time behavior, in which the system settles into either a stationary state that could be in or out of equilibrium and supports either global synchrony or absence of it, or, in a time-periodic synchronized state. We note that without noise ($T = 0$), the only possibility at long times would be given by all oscillators at the same position, either in a stationary state ($\Omega < W$) or in a time-periodic state ($\Omega > W$), thus a much less rich behavior. While we have an exact expression for the single-oscillator distribution in the stationary synchronized state (Eq. (5)) and in the stationary unsynchronized state (Eq. (7)), both obtained by solving the Fokker-Planck equation (4) in the stationary state, it is of interest to obtain the distribution in the time-periodic state by solving the full time-dependent Fokker-Planck equation. It would be also interesting to consider in place of the first-order dynamics (2) the corresponding second-order dynamics that accounts for the finite moment-of-inertia of the oscillators. In case of the Kuramoto model, the corresponding second-order dynamics leads to rather drastic consequences [28–31], and an issue would be to investigate how much of these are retained or modified by the presence of the local potential. Another interesting direction to pursue would be to consider the dynamics (2) with a non-mean-field coupling, i.e., with a coupling that decays as a power-law of the separation between oscillators occupying the sites of say a one-dimensional lattice [32].

Acknowledgements: We acknowledge fruitful discussions with S. Ruffo and A. Torcini. SG acknowledges financial support of INFN Roma and hospitality of Università di Roma "La Sapienza".

REFERENCES

[1] M. Bier, B. M. Bakker, and H. V. Westerhoff, Biophys. J. **78**, 1087 (2000).
[2] J. Buck, Quart. Rev. Biol. **63**, 265 (1988).
[3] S. Y. Ha, E. Jeong, and M. J. Kang, Nonlinearity **23**, 3139 (2010).
[4] A. T. Winfree, *The Geometry of Biological Time* (Springer, New York, 1980).
[5] G. Filatrella, A. H. Nielsen, and N. F. Pedersen, Eur. Phys. J B **61**, 485 (2008).
[6] I. Dobson, Nat. Phys. **9**, 133 (2013).
[7] A. Pikovsky, M. Rosenblum, and J. Kurths, *Synchronization: A Universal Concept in Nonlinear Sciences* (Cambridge University Press, Cambridge, 2001).
[8] S. H. Strogatz, *Sync* (Hyperion, New York, 2003).
[9] Y. Kuramoto, *Chemical oscillations, Waves and Turbulence* (Springer, Berlin, 1984).
[10] S. H. Strogatz, Physica D **143**, 1 (2000).
[11] J. A. Acebrón, L. L. Bonilla, C. J. P. Vicente, F. Ritort, and R. Spigler, Rev. Mod. Phys. **77**, 137 (2005).
[12] S. Gupta, A. Campa, and S. Ruffo, J. Stat. Mech.: Theory Exp. R08001 (2014).
[13] H. Sakaguchi, Prog. Theor. Phys. **79**, 39 (1988).
[14] S. H. Strogatz, C. M. Marcus, R. M. Westervelt, and R. E. Mirollo, Physica D **36**, 23 (1989).
[15] P. H. Chavanis, Eur. Phys. J. B **87**, 120 (2014).
[16] M. Antoni and S. Ruffo, Phys. Rev. E **52**, 2361 (1995).
[17] A. Campa, T. Dauxois, and S. Ruffo, Phys. Rep. **480**, 57 (2009).
[18] F. Bouchet, S. Gupta, and D. Mukamel, Physica A **389**, 4389 (2010).
[19] A. Campa, T. Dauxois, D. Fanelli, and S. Ruffo, *Physics of Long-range Interacting Systems* (Oxford University Press, Oxford, 2014).
[20] V. Privman, *Nonequilibrium Statistical Mechanics in One Dimension* (Cambridge University Press, Cambridge, 2005).
[21] E. Ott and T. M. Antonsen, Chaos **18**, 037113 (2008).
[22] L. M. Childs and S. H. Strogatz, Chaos **18**, 043128 (2008).
[23] J. Um, H. Hong, F. Marchesoni, and H. Park, Phys. Rev. Lett. **108**, 060601 (2012).
[24] P. Reimann, Phys. Rep. **361**, 57 (2002).
[25] D. Speer, R. Eichhorn, and P. Reimann, Europhys. Lett. **79**, 10005 (2007).
[26] O. E. Omel'chenko and M. Wolfrum, Phys. Rev. Lett. **109**, 164101 (2012).
[27] M. Komarov, S. Gupta, and A. Pikovsky, EPL **106**, 40003 (2014).
[28] S. Gupta, A. Campa, and S. Ruffo, Phys. Rev. E **89**, 022123 (2014).
[29] S. Olmi, A. Navas, S. Boccaletti, and A. Torcini, Phys. Rev. E **90**, 042905 (2014).
[30] S. Olmi and A. Torcini, in *Control of Self-Organizing Nonlinear Systems, Springer Series in Energetics*, edited by E. Schoell, S.H.L. Klapp, and P. Hoevel (Springer-Verlag, Berlin, 2016)
[31] A. Campa, S. Gupta, and S. Ruffo, J. Stat. Mech.: Theory Exp. P05011 (2015).
[32] S. Gupta, M. Potters, and S. Ruffo, Phys. Rev. E **85**, 066201 (2012); S. Gupta, A. Campa, and S. Ruffo, Phys. Rev. E **86**, 061130 (2012).